Published in final edited form as:
Dev Cell. 2013 December 9; 27(5): 545–559. doi:10.1016/j.devcel.2013.11.003.

FHOD1 is needed for directed Forces and Adhesion Maturation during Cell Spreading and Migration

Thomas Iskratsch[1,*], **Cheng-Han Yu**[2], **Anurag Mathur**[3,+], **Shuaimin Liu**[3], **Virginie Stévenin**[1], **Joseph Dwyer**[4], **James Hone**[3], **Elisabeth Ehler**[4], and **Michael Sheetz**[1,2,*]

[1]Biological Sciences, Columbia University, New York, NY, 10027, USA

[2]Mechanobiology Institute, National University of Singapore, Singapore, 117411, Singapore

[3]Department of Mechanical Engineering, Columbia University, New York, NY, 10027, USA

[4]Randall Division of Cell and Molecular Biophysics and Cardiovascular Division, King's College London, London, SE1 1UL, UK

Summary

Matrix adhesions provide critical signals for cell growth or differentiation. They form through a number of distinct steps that follow integrin binding to matrix ligands. In an early step, integrins form clusters that support actin polymerization by an unknown mechanism. This raises the question of how actin polymerization occurs at the integrin clusters. We report here that a major formin in mouse fibroblasts, FHOD1 is recruited to integrin clusters, resulting in actin assembly. Using cell-spreading assays on lipid bilayers, solid substrates and high-resolution force sensing pillar arrays, we find that knockdown of FHOD1 impairs spreading, coordinated application of adhesive force and adhesion maturation. Finally we show that targeting of FHOD1 to the integrin sites depends on the direct interaction with Src family kinases, and is upstream of the activation by Rho Kinase. Thus our findings provide insights into the mechanisms of cell migration with implications for development and disease.

Introduction

The events following fibroblast binding to and spreading on matrix-coated surfaces can be described by a series of sequential steps (Dubin-Thaler et al., 2008). The earliest events involve the clustering of the integrins to activate adhesion(Jiang et al., 2003). On solid substrates, integrin activation results in rapid spreading and adhesions mature over time through the contraction process(Cai et al., 2010; Giannone et al., 2004). In suspension cells, the binding of soluble ligand to integrins causes activation of Src family kinases (SFKs) (Huveneers and Danen, 2009), but the process stalls, because subsequent steps involve or

[*]To whom correspondence should be addressed: Thomas Iskratsch, Ph.D., Department of Biological Sciences, Columbia University, 715 Fairchild, 1212 Amsterdam Ave, New York, NY 10027, Phone 212-854-8002, FAX 212-854-6399, ti2170@columbia.edu; Michael Sheetz, Ph.D., William R. Kenan, Jr. Professor of Cell Biology, Department of Biological Sciences, Columbia University, 713 Fairchild, 1212 Amsterdam Ave, New York, NY 10027, Phone 212-854-4857, FAX 212-854-6399, ms2001@columbia.edu.
[+]Current address: Department of Bioengineering and California Institute for Quantitative Biosciences (QB3), University of California at Berkeley, Berkeley, Ca, 94720, USA

Supplemental Experimental Procedures: Additional experimental procedures can be found in the Supplemental Experimental Procedures, including the antibodies, sequences of the siRNAs and primers used in this work.

depend on surface forces. Recent studies of arginine-glycine-aspartic acid (RGD) ligands attached to mobile lipids with or without barriers to movement show that the initiation of spreading follows actin polymerization from clustered integrins, subsequent recruitment of myosin and force generation on the clusters(Yu et al., 2011). Actomyosin contractions of integrin clusters to the barriers are important to trigger further spreading by the previously reported pathways(Giannone et al., 2004). This raises the question of how actin polymerization occurs at the integrin clusters and whether it is downstream of Src family kinases. Since actin filament attachment to RGD-integrin clusters is critical for subsequent steps in the spreading process, we focus here on elucidating the mechanism of actin polymerization following integrin activation.

The ARP2/3 complex(Goley and Welch, 2006; Lai et al., 2008; Svitkina and Borisy, 1999), as well as several formins are detected in fibroblasts and associate with a range of actin structures, such as filopodia or stress fibers(Campellone and Welch, 2010; Mellor, 2010). Although the function of the ARP2/3 complex was closely linked to cell spreading, knockdown experiments or the use of specific ARP2/3 inhibitors indicate that additional actin assembly factors are involved in spreading (Di Nardo et al., 2005; Nolen et al., 2009; Steffen et al., 2006). In a screening of fibroblast actin assembly factors, we found localization of FHOD1 to early RGD clusters, while other prominent fibroblast formins, such as mDia1, mDia2 or FMNL3 were not targeted to the integrin sites. Indeed, FHOD1 is an interesting candidate for actin assembly from early integrin sites as it is a) regulated downstream of SFKs (Koka et al., 2005), even though details of the interaction remained unclear and b) FHOD1 has both, a barbed end elongation activity and a strong actin bundling activity (Schonichen et al., 2013). While in mature adhesions, actin filaments are bundled by α-actinin and other actin crosslinking proteins to ensure optimal force transmission (Roca-Cusachs et al., 2013; Roca-Cusachs et al., 2012), a combined elongation and bundling activity could guide assembly of contractile structures in the context of early integrin cluster formation.

To analyze a potential role of FHOD1 during early cell spreading we combined spreading assays on supported lipid bilayers and on rigid substrates, as well as on high precision force measuring pillar arrays. While spreading assays on rigid substrates are a well-established model for cell motility, the supported lipid bilayers provide an important contrast because they conserve steps of cell adhesion and spreading that occur prior to myosin contraction(Yu et al., 2011). Combining these methods, we provide evidence that FHOD1 is active at early integrin clusters that support actin polymerization. Further, the knockdown of FHOD1 causes an actin assembly defect from early adhesion sites and inhibits cell spreading through alterations in inwards traction stress and adhesion maturation. Finally, we find that the interaction between Src Family Kinases and FHOD1 is needed for adhesion targeting and subsequent activation.

Results

FHOD1 targets to early integrin clusters

In order to investigate a potential association of FHOD1 with early adhesions, we employed supported lipid membranes functionalized with RGD peptides, as the ligand for integrins. Two-dimensional mobility of the ligand on supported membranes enabled us to visualize the reorganization of activated integrins and the newly formed actin network associated with integrin clusters in live cells(Yu et al., 2011). FHOD1 is a low abundance protein and transfection resulted in a strong overexpression (Fig. S1a). Therefore, we focused on the analysis of low to moderately overexpressing cells. As cells started to adhere, fluorescently labeled RGD on supported bilayers formed submicron clusters. As soon as clusters were visible, ribbon-like polymerization of actin and FHOD1 binding were observed at RGD-

integrin clusters (Fig. 1a-b and Movie 1). As the clusters grew in size, the actin ribbons extended away (Fig. 1b-c, red arrowheads). The FHOD1 signal was more intense closer to the center of the clusters (Fig. 1b, green arrowheads, 1c, blue asterisks), but partially moving outwards with the actin, as well (Fig. 1c, red arrowheads). An enrichment of both FHOD1 and actin around RGD clusters was confirmed by plotting the averaged radial profiles of cells spread for 5 minutes (Fig. 1d-e). This behavior was specific for FHOD1, as other major fibroblast formins, such as mDia1, mDia2, or FMNL3 were not targeted to the clusters and localized diffusely to the cytoplasm (Fig. S2).

To exclude that this localization was an artifact of the lipid bilayer system, we next analyzed FHOD1's localization during cell spreading on fibronectin-coated coverslips. Cell spreading on rigid 2D surfaces was previously characterized by a phasic response that includes initial contact formation (or P0 phase), a fast increase in cell area driven by actin polymerization (P1) and periodic actomyosin contractions that propagate along the edge in lateral waves (P2) (Dobereiner et al., 2006; Dubin-Thaler et al., 2008; Giannone et al., 2007). The latter phase also includes the formation of early integrin adhesions along the cell edge, which mature over time. In our experiments, FHOD1-GFP showed a dynamic localization to actin structures in spreading fibroblasts during the P1 and P2 phase. The maximum intensity of the FHOD1 signal was observed behind the protruding cell edge (Movie 2 and Fig. 2a), close to the site of the lamellipodium-lamella interface. Additionally, in some instances FHOD1-GFP speckles appeared to be closer to the cell edge and inside the lamellipodium (Fig. 2b for kymograph and Fig. 2c for image sequence). FHOD1 aggregates grew in size over time before disappearing again as the cell protruded further. Such behavior was reminiscent of the formation of nascent adhesions in the lamellipodium, as well as their maturation at the boundary between lamellum and lamellipodium(Alexandrova et al., 2008). Indeed co-transfection with paxillin showed partial co-localization at nascent and mature focal adhesions (Fig. 2d).

Since the lipid bilayer experiments suggested that localization of FHOD1 to integrin clusters was independent of myosin-generated forces, we next analyzed the localization of FHOD1 in cells that were pre-treated with, and spread in the presence of blebbistatin. As reported previously(Choi et al., 2008), blebbistatin inhibited adhesion maturation and paxillin was found in nascent adhesions around the cell edge (Fig 2e). There, FHOD1 co-localized with paxillin, supporting the model that FHOD1 localization is independent of myosin II. In contrast, this localization was dependent on integrin activation by surface antigens, since no localization close to the cell edge was found when the cells were spread on poly-L-lysine (Fig 2f). Immunostaining with an anti-FHOD1 antibody confirmed the localization pattern to the tips of radial actin filaments (Fig 2g Fig. S1a). Interestingly, both transfected, as well as endogenous FHOD1 were at least partially detected in a periodic pattern along the actin filaments, which could be related to an actin bundling activity (Schonichen et al., 2013).

We next sought to analyze if FHOD1 was active during early cell spreading and thus could be involved in actin assembly at the early integrin clusters and adhesions. Formins of the FHOD subfamily are known to be activated by phosphorylation of a consensus sequence in the DAD domain by Rho Kinase (ROCK), which results in the release of the auto-interaction and promotion of actin assembly(Iskratsch et al., 2013; Takeya et al., 2008). Using a phosphospecific antibody (Fig. 2h, Fig. S1c-e) we found the peak of FHOD1 activity 3 to 8 minutes after cell plating, and thus at times where the majority of cells started to form adhesions at the cell edge.

FHOD1 knockdown inhibits cell spreading

To further test if FHOD1 was required during early cell spreading for the actin assembly from adhesion sites, we designed shRNA constructs against FHOD1 (Fig S1b). FHOD1

knockdown cells formed filopodia, but failed to form coherent protrusions and spread in a segmented fashion (Fig. 3a, and Movie 3 and 4). Frequently, protrusions were not stable and collapsed entirely (arrows in Fig. 3a). Moreover, the speed of cell spreading was strongly reduced (Fig. 3b). Cell area, shape and F-actin content were restored to normal levels by co-expression of siRNA-resistant human FHOD1 (Fig. S3). Similarly, treatment with the pan-formin inhibitor smiFH2 impaired cell spreading in a dose dependent manner (Fig. S4), thus confirming the requirement for formin family proteins for early cell spreading.

FHOD1 knockdown suppresses focal adhesion formation

Since FHOD1 localized to early adhesions and protrusions in knockdown cells were less stable, we tested if there was a defect in focal adhesion formation. For this we knocked down FHOD1 for 72 hours and then additionally transfected the cells with Paxillin-GFP and pRuby-Lifeact and imaged the cells for > 20 minutes starting with the fast spreading phase (P1) to observe the adhesion formation during the protrusion-retraction phase. During the outward spreading, control cells formed nascent adhesions, many of which matured to focal adhesions after the transition to the protrusion-retraction phase (Fig. 3c-d and Movie 5). Again FHOD1 knockdown cells formed protrusions that frequently collapsed. Although knockdown cells initially formed nascent adhesions as well, they did not mature and eventually turned over (see kymograph in Fig. 3d). Additionally, the actin filament density and organization was reduced in knockdown cells (Fig. 3c and Fig. S5a-b). We further confirmed a defect in adhesion formation by immunostaining with an anti-paxillin antibody (Fig 3e). Quantification of the adhesion area showed a significant reduction in FHOD1 knockdown cells and a concomitant increase in the fraction of nascent adhesions (Fig. 3f-g). Again, treatment with the pan-formin inhibitor showed a similar reduction in adhesion size and F-actin density (Fig. S5c). Immunostaining for active β1-integrin (9EG7) showed that the FHOD1 knockdown did not affect the integrin activation at the cell edge, suggesting that FHOD1 acted downstream of integrin engagement (Fig 3h). However, both total and active β1-integrin signals were limited to the cell edge, further documenting the defect in adhesion maturation.

FHOD1 knockdown impairs cell migration

Cell spreading assays are commonly used as model system for motility experiments and especially for adhesion formation. The highly reproducible sequence of functional phases had in the past led to many important insights (Dobereiner et al., 2006; Dubin-Thaler et al., 2008; Giannone et al., 2004; Giannone et al., 2007). Nevertheless, to confirm that FHOD1's role in adhesion formation had a broader relevance for cell migration, we performed wound scratch assays in control and FHOD1 knockdown cells (Fig. 3i-l). After application of a wound with a pipette tip, control cells started to migrate quickly towards the center of the wound and the wound was closed within approximately 24h. FHOD1 knockdown cells, in contrast, migrated slowly and only a third of the wound was closed within 24h (Fig. 3j-k). When we fixed the cells after 8 hours, we found that similar to the spreading assays, FHOD1 knockdown cells lacked strong, polarized actin filaments and adhesions were frequently limited to the periphery and had a dot-like appearance (Fig. 3l). Within the first 50 μm from the leading edge (i.e. approx. the first row of cells), the cell area occupied by adhesions was reduced from 17.0% ± 1.3 to 6.7% ± 0.4 (n=14 images with ~ 5 cells each from 3 experiments, $p<0.0001$). This suggested that impaired adhesion formation was a general characteristic of FHOD1 knockdown cells which contributes to spreading, as well as migration defects (Fig. 3l).

FHOD1 is necessary for effective force transmission at integrin adhesions

The lack of adhesion maturation suggested a potential defect in the force coupling at the adhesion. Therefore we plated cells on sub-micron PDMS pillar arrays that enabled non-

disruptive live imaging of localized traction forces(Ghassemi et al., 2012). Surprisingly, there was a complete lack of coordinated inward forces in knockdown cells. While in control cells whole rows of pillars were displaced perpendicular to the cell edge over tens of seconds, pillar displacement magnitude and angles fluctuated wildly in knockdown cells (Fig 4a-c, Movie 6). As a result, the maximum inwards traction stress (vector component perpendicular to the cell edge) was significantly reduced from 1440 ± 35.44 pN/μm^2 to 1180 ± 37.02 pN/μm^2 (Fig. 4d) and even more strikingly the overall inward traction was lost (average traction stress, Fig. 4e). It is noteworthy that the maximum pillar displacement values remained unchanged (data not shown), suggesting that there was a loss of organization but not of force production in absence of FHOD1.

The fact that the traction forces were present only as short bursts that changed magnitude and direction quickly, indicated that myosins were pulling from multiple directions (see working model in Figure 5a). As a result, the forces were not directed and ultimately canceled each other out (Fig 4c,e). An expected consequence of this finding was a reduction in the retrograde flow and more off-axis movements. To test this prediction, we analyzed the retrograde flow by observing the behavior of fibronectin-coated beads (1 μm diameter) that were placed at the cell edge with the help of an optical trap (Choquet et al., 1997). Indeed, in FHOD1 knockdown cells, beads were transported inward at an overall slower pace and with many random off-axis movements (Fig 5b-d, Movie 7).

FHOD1 knockdown cells on RGD supported membranes showed also reduced actin polymerization from RGD-integrin clusters, as well as reduced cluster growth. There was no, or only slow active actin polymerization or expansion outward from the clusters in FHOD1 knockdown cells (Fig. 6a-b/Movie 8). RGD clusters frequently had no overlapping Lifeact signal (such as indicated by red arrows in Fig. 6a) and the Lifeact signal was also detected in areas where no RGD clustering was detected (yellow arrows). Further, plotting of the average radial profiles and quantification of the integrated density over a radius of 2.5 μm from the center of the clusters showed a significant decrease of the Lifeact and RGD fluorescence intensity (Fig. 6c-e). Thus, the knockdown of FHOD1 inhibited actin assembly from early integrin clusters and further impaired cluster maturation.

Together these results indicated that FHOD1 was recruited to early integrin clusters downstream of receptor-ligand clustering, but independent of force. Further, it was instrumental in organizing the actin for efficient force coupling at the adhesions and thus facilitated continued cluster growth.

FHOD1 interaction with SFKs is necessary for its activation

Recent findings showed that the SFK inhibitor PP2 inhibited actin polymerization from early integrin clusters(Yu et al., 2011). Moreover, it was shown that FHOD1 was regulated downstream of SFKs since treatment with the Src inhibitor PP2 abolished the FHOD1-induced transcription of the skeletal actin promoter(Koka et al., 2005). If FHOD1 played a role in the actin organization at integrin clusters, SFKs were possibly involved in the targeting of FHOD1 to integrin sites. Therefore, we analyzed targeting of FHOD1 to RGD-integrin clusters in PP2-treated fibroblasts. As reported previously(Yu et al., 2011), the PP2 treatment reduced growth of the integrin clusters. Further, no ribbon-like polymerization of actin was detected and enrichment of FHOD1 around the clusters was reduced (Fig. S6).

FHOD1 contains a conserved YEEI sequence on its N-terminus (^{99}YEEI) that, when phosphorylated constitutes a strong Src SH2 binding motif (Songyang et al., 1993)(Fig. 7a). Additionally, the poly-proline stretch of the FH1 domain is a putative SH3 binding site(Jia et al., 2005; Roskoski, 2004). Indeed, we confirmed tyrosine phosphorylation of immunoprecipitated full-length FHOD1, which was absent in a tyrosine to phenylalanine

mutant (Y99F), and also lost after deletion of the poly-proline region (Δpoly-Pro) (Fig. 7b). Further, SFKs co-precipitated with FHOD1, but the binding was reduced in case of the Y99F mutation and absent in the case of the Δpoly-proline mutation. Moreover, both mutations led to a loss of FHOD1 activity, as measured by Thr1141 phosphorylation, thus indicating that the interaction with SFKs via the poly-proline region resulted in tyrosine (Y99) phosphorylation, stronger SFK binding and downstream activation of FHOD1.

To further investigate the interaction with SFKs, we used mouse fibroblast cells deficient in Src, Yes and Fyn (SYF cells)(Klinghoffer et al., 1999), as well as SYF cells that had Src re-introduced by retroviral transduction or were stably transfected with either Yes or Fyn. Interestingly, co-precipitation of the SFKs and partial restoration of tyrosine and Thr1141 phosphorylation were detected with all three kinases, but only Src restored the phosphorylation to the control levels (Fig. 7c). However, due to the retroviral transduction, as opposed to the stable transfection, Src levels exceeded those of the other kinases.

If SFKs were upstream of FHOD1 activation, knockdown of FHOD1 should not affect the spreading phenotype of SYF cells. In line with previous results (Cary et al., 2002; Klinghoffer et al., 1999; Kostic and Sheetz, 2006; von Wichert et al., 2003), SYF cells showed aberrant spreading behavior and reduced adhesion formation. Thus, the cells exhibited several similarities with FHOD1 knockdown cells, such as reduced cell area (Fig. 7d-e), segmented cell morphology (Fig. 7f), reduced adhesion area and an increased number of small adhesions after 30 minutes of spreading (<0.2 μm^2, Fig. 7g). FHOD1 knockdown in SYF cells however did not result in an aggravation of any of the spreading defects, indicating that FHOD1 was downstream of SFKs.

Targeting to adhesion sites is controlled by Src Family Kinases

Because both the Y99F and the Δpoly-Pro lacked Thr1141 phosphorylation (and hence were inactive) and FHOD1 binding to RGD clusters was reduced after PP2 treatment, we hypothesized that the interaction with SFKs was necessary for correct targeting to the integrins and subsequent activation by ROCK. Indeed, the typical localization pattern of FHOD1 with Paxillin was lost in the SYF cells and was partially restored in all three SYF add back cell lines (Fig. 8a). Also, localization of the Y99F mutant to the adhesions was reduced and no overlap between FHOD1-Δpoly-Pro-GFP and Paxillin was found (Fig. 8b,d), while a constitutive inactive mutant of the ROCK phosphorylation sites (FHOD1-3A) still localized to the adhesions. Co-localization with actin decreased both with FHOD1-3A and the Δpoly-proline mutation, which was presumably due to a loss of actin filaments in these cells (Fig. 8c,e). Indeed, transfection with FHOD1-Δpoly-Pro-GFP induced a phenotype similar to a FHOD1 knockdown. Cells were depleted of actin filaments and lacked strong adhesions. In lipid bilayer experiments, the Δpoly-Pro mutant inhibited spreading entirely in approximately 40% of the cells. In the remaining cells, only small amounts of FHOD1 Δpoly-Pro were found around the RGD clusters and the clusters lacked the typical ribbon-like actin polymerization (Fig. 8f-i), indicating that the poly-proline deletion mutant sequestered endogenous FHOD1 away from the RGD clusters. Similarly, FHOD1-Y99F localization to the clusters was reduced and no Lifeact enrichment was found around the clusters. FHOD1-3A in contrast showed no targeting defect to the RGD clusters and actin enrichment was only slightly reduced (Fig. 8h-i, not significant), indicating that this mutant did not display a dominant phenotype.

Together the data indicated that SFKs bound to the FHOD1 poly-proline region, which resulted in phosphorylation of the YEEI motif and increased interaction with Src kinases. These events were necessary for the correct targeting of FHOD1 to integrins and its activation, which enabled actin polymerization from integrin clusters during cell spreading and migration.

Discussion

In the present study, we combine the supported lipid bilayer system with high-resolution force sensing pillar arrays and well-established cell spreading and migration assays on solid substrates to study actin assembly from early integrin clusters and subsequent adhesion formation. Importantly, since supported bilayers provide an environment where there is no in-plane resistance to movement and thus provide an important contrast to planar glass substrates (Yu et al., 2011), we are able to characterize steps during adhesion formation that are prior to myosin activity. Sub-micron elastomer pillars on the other hand allow us to analyse localized traction stress with high precision. Using these methods we show here that the formin family protein FHOD1 is critical for actin assembly from integrin clusters, inward-directed traction stress as well as cell spreading and adhesion maturation. This is consistent with the hypothesis that the early spreading involves actin polymerization from ligand-bound integrin clusters to enable myosin-dependent cluster growth and further spreading through lamellipodial extension(Yu et al., 2011).

Further, our results show that FHOD1 is required to form actin structures that allow effective coupling of myosin traction forces to the adhesion. Without FHOD1, forces on adhesion sites are present only as short bursts and not directed. Since there are other actin assembly proteins present at (e.g. VASP(Worth et al., 2010)) or close to adhesions (e.g. ARP2/3), actin filaments are still formed in the absence of FHOD1, albeit to lower extents. However, without FHOD1 there is a lack of actin organization. This is in agreement with an actin bundling function, which was reported previously (Schonichen et al., 2013). Indeed, in lipid bilayer experiments, a part of the GFP tagged FHOD1 moved outward from the integrin clusters, together with the polymerizing actin. Moreover, we also detected FHOD1 in a periodic pattern on fibronectin-coated glass, which could further indicate such bundling activity.

While the in-vitro work by Schönichen and co-workers found that FHOD1 lacks actin nucleation activity and only displays weak filament elongation activity, other studies reported that FHOD1 enhanced actin polymerization in cyto (Gasteier et al., 2003; Gasteier et al., 2005; Koka et al., 2005; Watanabe et al., 1999), suggesting that FHOD1 might elongate previously nucleated filaments. Similarly, some of our results - especially the decreased actin polymerization from early integrin clusters in FHOD1 knockdown cells, or in presence of the delta-polyPro or the Y99F mutant, clearly point towards an active actin elongation by FHOD1 during early spreading.

Independent of a bundling or elongation activity, our data shows clearly that FHOD1 is targeted to integrin adhesions downstream of Src Family Kinases. Subsequently it appears to be activated by ROCK to enable actin assembly from integrin clusters and cell spreading. This is in support of the proposed model that formin localization and activation are separate phenomena (Ramalingam et al., 2010).

While it has been shown previously that FHOD1 is activated by ROCK (Hannemann et al., 2008; Schulte et al., 2008; Takeya et al., 2008) and regulated downstream of SFKs (Koka et al., 2005), details of the mechanism remained unclear. We confirm here that the activation is downstream of SFKs in several ways: 1) abolishing the interaction by incubation with PP2, 2) using SYF cells or 3) mutation of the interaction sites all reduce activation of FHOD1. In contrast, a constitutive inactive mutant (FHOD1-3A)(Takeya et al., 2008) can still localize to the adhesion regions. Further, binding of Src to the poly-proline region, followed by phosphorylation of a YEEI sequence on the N-terminus enables the subsequent activation. FH1-SH3 domain interactions have been reported previously for yeast and trematode formins(Kamei et al., 1998; Quack et al., 2009) and a similar mechanism has been detected

also for other proteins, such as p130Cas, where the interaction between the poly-proline region and the Src SH3 domain serves to activate Src and results in subsequent phosphorylation of p130Cas(Bibbins et al., 1993; Pellicena and Miller, 2001; Pellicena et al., 1998). The interaction with SFKs might bring FHOD1 in close proximity to ROCK at the membrane(Riento and Ridley, 2003) and thus enables the activation. During cell spreading this results in a peak of FHOD1 activity at a time when the majority of cells form new adhesions all around the cell edge. While at later time points during spreading (and also migration) nascent adhesions are formed as well; but only a small portion of the edge moves out at any time (not all around the cell edge and in a large fraction of the spreading cells). Therefore FHOD1 phosphorylation returns to the base line levels in spread cells. Rapid and transient phosphorylation of FHOD1 after receptor engagement was also found in other cell types, i.e. after collagen related peptide (CRP) stimulation in human platelets(Thomas et al., 2011) and could mark a universal event in the stimulation of actin polymerization upon integrin clustering.

Our results show that only Src can efficiently phosphorylate FHOD1 at Y99 to enable the downstream activation by ROCK. However, in Yes and Fyn add back cells, the expression levels of the respective SFKs are lower than in wild type cells and thus the SFK activity might not be sufficient for a full recovery of FHOD1 phosphorylation on a cellular level, but rather only lead to localized effects. Indeed, our results suggest that add back of Yes or Fyn is sufficient to restore the targeting at least partially. Nevertheless, we cannot exclude that these effects on adhesion targeting are only due to a redundancy between the SFKs (Lowell and Soriano, 1996).

Together our study shows that FHOD1 is a critical actin assembly factor at the early integrin clusters during cell spreading and migration and it triggers a cascade of events that eventually produces longer term adhesions through the polymerization and bundling of actin filaments.

Although several formins that were previously studied in fibroblasts participate in adhesion formation and/or maturation (Goode and Eck, 2007; Gupton et al., 2007; Yamana et al., 2006), our study shows specific targeting of a formin to integrin adhesions. Further, our data shows that this targeting depends on integrin-ligand engagement, but not myosin contractility. This could be important since recent findings have highlighted the role of mammalian and yeast formins as mechanosensors (Courtemanche et al., 2013; Higashida et al., 2013; Jegou et al., 2013). In these studies, formin activity was enhanced in presence of profilin by a pulling force on tethered mDia1 or Bni1p in flow chambers and on membrane bound mDia1 in cells. Although it remains to be seen if the same applies to FHOD1, a force dependent regulation of an adhesion localized actin assembly factor would provide a direct link between integrin mechanosensing and actin driven cell protrusion.

Experimental Procedures

Cell culture and transfections

RPTPα+/+ mouse embryonic fibroblast (MEF) cells and SYF cells were cultured in DMEM with 10% fetal bovine serum and 1% penicillin/streptomycin to 70%-80% confluency and passaged the day before the experiment. If not indicated otherwise, cells were transfected for 24hours with an AMAXA nucleofector using the MEF transfection KIT (Lonza) according to the manufacturer's instructions. SYF+Src cell were obatined from ATCC, SYF+Fyn and SYF+Yes add-back cells were a kind gift from Dr. Yasuhiro Sawada.

Microscopy

DIC and bright field time-lapse imaging was performed with an Olympus IX-70 inverted microscope maintained at 37 °C using a 100x N.A. 140, 60× N.A. 1.40 or a 20x N.A. 1.40 oil objective (all Olympus), a CoolSNAP HQ (Photometrics) CCD camera and micro-manager or MetaMorph microscopy software (Molecular Devices).

TIRF images and time-lapse micrographs were taken using an Olympus IX81 fluorescence microscope maintained at 37 °C with a 60× N.A. 1.45 objective and a Cool Snap FX cooled CCD camera (Photometrics) controlled by SimplePCI (Compix Inc.) software. Confocal microscopy was performed on a Zeiss LSM700 laser-scanning confocal microscope using a 63x N.A. 1.40 objective (Zeiss) or an Olympus Fluoview FV500 laser-scanning confocal microscope using a 60x N.A. 1.40 objective (Olympus).

Spreading assays

Cells were spread on human plasma full-length pure fibronectin (10 μg/ml, Roche) coated sialinized cover glasses, or for western blotting and immunoprecipitation assays on fibronectin-coated tissue culture dishes. Cells were trypsinized, washed with Soybean trypsin inhibitor, centrifuged and pre-incubated in Ringer medium (150 mM NaCl, 5 mM KCl, 1 mM $CaCl_2$, 1 mM $MgCl_2$, 20 mM Hepes and 2g/L D-Glucose at pH 7.4) for 30 minutes prior to the experiment. Cells were plated and imaged by time-lapse microscopy (DIC or TIRF), or fixed with 4% paraformaldehyde/PBS and stained for confocal microscopy. For western blotting and co-immunoprecipitation assays, cells were lysed in (20 mM TRIS, 137 mM NaCl, 10% Glycerol and 1% NP40 at pH8.0, including protease and phosphatase inhibitor cocktails (cOmplete EDTA free Protease Inhibitor Cocktail Tablets and PhosSTOP Phosphatase Inhibitor Cocktail Tablets, both Roche) on ice, snap frozen, rethawed and cleared from cell debris by centrifugation. In case of smiFH2 (Sigma), Blebbistatin (Sigma) or Y-27632 (Tocris) treatment, indicated doses of drugs were present during the pre-incubation, as well as the spreading experiment. For FHOD1-GFP immunoprecipitations we used the Crosslink immunoprecipitation Kit (Pierce) and monoclonal mouse anti-GFP (Roche) antibody.

Analysis of edge velocities

Spread area was calculated with the “Analyze Particles” function of ImageJ, after using the “Find Edges” function and thresholding to binarize the cells. Where necessary, “Close”, “Fill Holes” and “Remove Outliers” functions were used to receive a coherent mask of the cell. Outlines of the measured cells were added to the original image series with the “Image Calculator” function as a control. Spread phases were identified after plotting the logarithm of the area vs. the logarithm of the time(Dubin-Thaler et al., 2008)(see also Fig. S1a). Average edge velocities were calculated as the slope of the radius of a circle with the measured cell area over the time.

Wound healing assays

Cells were transfected with FHOD1 shRNA or Control shRNA plasmids and cultured for 96 hours in the presence of 150 μg/ml zeozin. Subsequently, cells were plated to confluency on fibronectin coated tissue culture, or if intended for immunofluorescence, on fibronectin coated glass bottom dishes (MatTek). After 12 hours, a wound was applied with a pipette tip, cells were washed twice with fresh full medium and marked areas were imaged every 8 hours with a Olympus IX81 fluorescence microscope maintained at 37 °C with a 10x N.A. 0.3 objective (Olympus). The (paxillin) adhesion area was measured with ImageJ within a 50 μm wide ROI, after thresholding and using the “analyze particle” function. Regions with a strong, diffuse cytoplasmic paxillin signal were excluded from the analysis.

Traction force measurements

Pillar arrays (1.1 μm in height, 0.5 μm diameter, 1 μm center to center, k=13.9 nN/μm) coated with 10 μg/ml of fibronectin (Invitrogen) were prepared as described previously(Ghassemi et al., 2012). Briefly, cells were spread on pillar arrays and bright field movies were taken as described above with a frame rate of one frame per second. Displacements were measured with imageJ, using the NanoTracking plugin.

Bead displacement analysis

1μm diameter silica microspheres (Bangs Laboratories) were activated with cyanogen bromide and covalently labelled with fibronectin according to the manufacturers instructions (TechNote 205). Cells (Control and FHOD1 shRNA transfected for 4 days) and beads were added onto fibronectin coated coverslips. Beads were placed at the edge of cells with an optical trap, using a 2W diode pumped 1064nm laser (CrystalLaser) until they were fixed on the cell surface (i.e. the optical trap force was unable to produce a detectable movement of the bead) and visualized with a 100× N.A. 1.3 objective on an inverted Axiovert 100 TV microscope, equipped with Nomarsky optics. After thresholding, beads were tracked with ImageJ (Fiji) using the MTrack2 plugin.

Functionalized supported lipid bilayer membrane

RGD peptide, a biotinylated peptide of cyclo [Arg-Gly-Asp-D-Phe-Lys(Biotin-PEG-PEG)], was purchase from Peptides International (3697-PI, Louisville, KY, USA). 1,2-dioleoyl-sn-glycero-3-phosphocholine (DOPC) and 1,2-dipalmitoyl-sn-glycero-3-phosphoethanolamine-N-(cap biotinyl) (16:0 biotinyl-Cap-PE) were purchased from Avanti Polar Lipids (Alabaster, AL, USA). Cascade Blue neutravidin was purchased from Invitrogen (Carlsbad, CA, USA). Detailed preparation methods were previously described(Yu et al., 2011). In brief, small lipid vesicles (0.4 mol% of biotinyl-Cap-PE and 99.6 mol% of DOPC) were made by sonication and then were used to deposit onto glass cover glass under aqueous condition with 150mM phosphate buffered saline in room temperature. Neutravidin serves as the link between biotinyl-Cap-PE and biotinylated RGD peptide. 1μg/mL of fluorescently-labeled neutravidin (Cascade Blue) was added onto supported lipid membranes for 30-minutes incubation. After washing off excess neutravidin, 1μg/mL of biotinylated RGD was added to neutravidin-coated supported membranes for another 30-minute. Excess RGD was removed by serial solvent exchange, 25mL of 150mM PBS in each chamber, and then 15mL of serum-free DMEM media. In general, the two-dimensional diffusion coefficient of RGD-supported membrane is measured as high as 2.5 $\mu m^2/s$.

RGD cluster analysis

A tiff stack of RGD clusters from cells that were spread for five minutes was created and the average image calculated with ImageJ. A circular ROI with a radius of 2.5 μm was drawn around the center of the clusters. To analyze the enrichment of proteins around the clusters, we subtracted the average pixel intensity outside the ROI from each channel. The resulting image was used to quantify the integrated intensity of each channel and create radial profiles with ImageJ, using the Radial Profile Plot plugin. The data is presented as the radial profile of the average over all clusters for a certain condition, as well as the mean integrated intensities (+/- standard deviation) of the average clusters from single cell

Immunofluorescence

Fixed cells were permeabilized with 0.2% Triton X-100 in PBS for 5 minutes, or 0.02% Triton for 5 minutes for the integrin staining, blocked with MAXblock blocking medium (Active Motif) according to the manufacturers instruction and stained with the primary antibody mix in immunostaining buffer (1% BSA, 20 mM Tris-base, 155 mM NaCl, 2 mM

EGTA, and 2 mM MgCl2, pH 7.5) for one hour under shaking at room temperature. Cells were washed three times with PBS and incubated with the secondary antibody mix, containing Phalloidin (Alexa Fluor 546 or Alexa Fluor 633-Phalloidin, Invitrogen) where indicated. After washing three times with PBS, cells were mounted in 0.1 M Tris-HCl/glycerol (3:7) and 50 mg/ml N-propyl-gallate, pH 9.5.

Statistical testing

In the current study, two-tailed Student's t-test was used for comparison between two groups. Data sets were tested for normal distribution using the Shapiro–Wilk test. If not stated otherwise, all box plots are displayed as median (central line), upper and lower quartile (box), +/- 1.5 x inter quartile range (whiskers) with outliers displayed separately. Two-way analysis of variance (ANOVA) and Bonferroni posttests were calculated with Graphpad Prism 5.

Image processing

Original digital images obtained were assembled to the figures and labeled using Indesign or Illustrator (Adobe). Only linear contrast adjustments were used and were always applied to the entire image.

Supplementary Material

Refer to Web version on PubMed Central for supplementary material.

Acknowledgments

We are grateful to Prof. Yasuhiro Sawada for the SYF add-back cell lines. We also like to thank Prof. Reuven Agami for providing pSUPER, Prof. Anne Ridley for FMNL3, Prof. Arthur Alberts for mDia2, Prof. Roland Wedlich-Söldner for Lifeact and Prof. Partridge for the Paxillin plasmids. We gratefully acknowledge the help of Miss Lale Alpar and the critical reading and helpful comments provided by Dr. Nicolas Biais and Dr. Haguy Wolfenson. This work was supported by NIH grant EB001480, as well as EY016586

References

Alexandrova AY, Arnold K, Schaub S, Vasiliev JM, Meister JJ, Bershadsky AD, Verkhovsky AB. Comparative dynamics of retrograde actin flow and focal adhesions: formation of nascent adhesions triggers transition from fast to slow flow. PLoS One. 2008; 3:e3234.

Bibbins KB, Boeuf H, Varmus HE. Binding of the Src SH2 domain to phosphopeptides is determined by residues in both the SH2 domain and the phosphopeptides. Mol Cell Biol. 1993; 13:7278–7287. [PubMed: 7504171]

Cai Y, Rossier O, Gauthier NC, Biais N, Fardin MA, Zhang X, Miller LW, Ladoux B, Cornish VW, Sheetz MP. Cytoskeletal coherence requires myosin-IIA contractility. J Cell Sci. 2010; 123:413–423. [PubMed: 20067993]

Campellone KG, Welch MD. A nucleator arms race: cellular control of actin assembly. Nat Rev Mol Cell Biol. 2010; 11:237–251. [PubMed: 20237478]

Cary LA, Klinghoffer RA, Sachsenmaier C, Cooper JA. SRC catalytic but not scaffolding function is needed for integrin-regulated tyrosine phosphorylation, cell migration, and cell spreading. Mol Cell Biol. 2002; 22:2427–2440.

Choi CK, Vicente-Manzanares M, Zareno J, Whitmore LA, Mogilner A, Horwitz AR. Actin and alpha-actinin orchestrate the assembly and maturation of nascent adhesions in a myosin II motor-independent manner. Nature cell biology. 2008; 10:1039–1050.

Choquet D, Felsenfeld DP, Sheetz MP. Extracellular matrix rigidity causes strengthening of integrin-cytoskeleton linkages. Cell. 1997; 88:39–48. [PubMed: 9019403]

Courtemanche N, Lee JY, Pollard TD, Greene EC. Tension modulates actin filament polymerization mediated by formin and profilin. Proc Natl Acad Sci U S A. 2013; 110:9752–9757. [PubMed: 23716666]

Di Nardo A, Cicchetti G, Falet H, Hartwig JH, Stossel TP, Kwiatkowski DJ. Arp2/3 complex-deficient mouse fibroblasts are viable and have normal leading-edge actin structure and function. Proc Natl Acad Sci U S A. 2005; 102:16263–16268. [PubMed: 16254049]

Dobereiner HG, Dubin-Thaler BJ, Hofman JM, Xenias HS, Sims TN, Giannone G, Dustin ML, Wiggins CH, Sheetz MP. Lateral membrane waves constitute a universal dynamic pattern of motile cells. Phys Rev Lett. 2006; 97:038102. [PubMed: 16907546]

Dubin-Thaler BJ, Hofman JM, Cai Y, Xenias H, Spielman I, Shneidman AV, David LA, Dobereiner HG, Wiggins CH, Sheetz MP. Quantification of cell edge velocities and traction forces reveals distinct motility modules during cell spreading. PLoS One. 2008; 3:e3735. [PubMed: 19011687]

Gasteier JE, Madrid R, Krautkrämer E, Schröder S, Muranyi W, Benichou S, Fackler OT. Activation of the Rac-binding partner FHOD1 induces actin stress fibers via a ROCK-dependent mechanism. J Biol Chem. 2003; 278:38902–38912. [PubMed: 12857739]

Gasteier JE, Schroeder S, Muranyi W, Madrid R, Benichou S, Fackler OT. FHOD1 coordinates actin filament and microtubule alignment to mediate cell elongation. Exp Cell Res. 2005; 306:192–202. [PubMed: 15878344]

Ghassemi S, Meacci G, Liu S, Gondarenko AA, Mathur A, Roca-Cusachs P, Sheetz MP, Hone J. Cells test substrate rigidity by local contractions on submicrometer pillars. Proc Natl Acad Sci U S A. 2012

Giannone G, Dubin-Thaler BJ, Dobereiner HG, Kieffer N, Bresnick AR, Sheetz MP. Periodic lamellipodial contractions correlate with rearward actin waves. Cell. 2004; 116:431–443. [PubMed: 15016377]

Giannone G, Dubin-Thaler BJ, Rossier O, Cai Y, Chaga O, Jiang G, Beaver W, Dobereiner HG, Freund Y, Borisy G, et al. Lamellipodial actin mechanically links myosin activity with adhesion-site formation. Cell. 2007; 128:561–575. [PubMed: 17289574]

Goley ED, Welch MD. The ARP2/3 complex: an actin nucleator comes of age. Nat Rev Mol Cell Biol. 2006; 7:713–726. [PubMed: 16990851]

Goode BL, Eck MJ. Mechanism and function of formins in the control of actin assembly. Annu Rev Biochem. 2007; 76:593–627. [PubMed: 17373907]

Gupton SL, Eisenmann K, Alberts AS, Waterman-Storer CM. mDia2 regulates actin and focal adhesion dynamics and organization in the lamella for efficient epithelial cell migration. J Cell Sci. 2007; 120:3475–3487. [PubMed: 17855386]

Hannemann S, Madrid R, Stastna J, Kitzing T, Gasteier J, Schönichen A, Bouchet J, Jimenez A, Geyer M, Grosse R, et al. The Diaphanous-related Formin FHOD1 associates with ROCK1 and promotes Src-dependent plasma membrane blebbing. J Biol Chem. 2008; 283:27891–27903. [PubMed: 18694941]

Higashida C, Kiuchi T, Akiba Y, Mizuno H, Maruoka M, Narumiya S, Mizuno K, Watanabe N. F- and G-actin homeostasis regulates mechanosensitive actin nucleation by formins. Nature cell biology. 2013; 15:395–405.

Huveneers S, Danen EH. Adhesion signaling - crosstalk between integrins, Src and Rho. J Cell Sci. 2009; 122:1059–1069. [PubMed: 19339545]

Iskratsch T, Reijntjes S, Dwyer J, Toselli P, Degano IR, Dominguez I, Ehler E. Two distinct phosphorylation events govern the function of muscle FHOD3. Cell Mol Life Sci. 2013; 70:893–908. [PubMed: 23052206]

Jegou A, Carlier MF, Romet-Lemonne G. Formin mDia1 senses and generates mechanical forces on actin filaments. Nat Commun. 2013; 4:1883. [PubMed: 23695677]

Jia CY, Nie J, Wu C, Li C, Li SS. Novel Src homology 3 domain-binding motifs identified from proteomic screen of a Pro-rich region. Mol Cell Proteomics. 2005; 4:1155–1166. [PubMed: 15929943]

Jiang G, Giannone G, Critchley DR, Fukumoto E, Sheetz MP. Two-piconewton slip bond between fibronectin and the cytoskeleton depends on talin. Nature. 2003; 424:334–337. [PubMed: 12867986]

Kamei T, Tanaka K, Hihara T, Umikawa M, Imamura H, Kikyo M, Ozaki K, Takai Y. Interaction of Bnr1p with a novel Src homology 3 domain-containing Hof1p. Implication in cytokinesis in Saccharomyces cerevisiae. The Journal of biological chemistry. 1998; 273:28341–28345. [PubMed: 9774458]

Klinghoffer RA, Sachsenmaier C, Cooper JA, Soriano P. Src family kinases are required for integrin but not PDGFR signal transduction. The EMBO journal. 1999; 18:2459–2471. [PubMed: 10228160]

Koka S, Minick GT, Zhou Y, Westendorf JJ, Boehm MB. Src regulates the activity of the mammalian formin protein FHOD1. Biochem Biophys Res Commun. 2005; 336:1285–1291. [PubMed: 16169515]

Kostic A, Sheetz MP. Fibronectin rigidity response through Fyn and p130Cas recruitment to the leading edge. Mol Biol Cell. 2006; 17:2684–2695. [PubMed: 16597701]

Lai FP, Szczodrak M, Block J, Faix J, Breitsprecher D, Mannherz HG, Stradal TE, Dunn GA, Small JV, Rottner K. Arp2/3 complex interactions and actin network turnover in lamellipodia. Embo J. 2008; 27:982–992. [PubMed: 18309290]

Lowell CA, Soriano P. Knockouts of Src-family kinases: stiff bones, wimpy T cells, and bad memories. Genes Dev. 1996; 10:1845–1857. [PubMed: 8756343]

Mellor H. The role of formins in filopodia formation. Biochim Biophys Acta. 2010; 1803:191–200. [PubMed: 19171166]

Nolen BJ, Tomasevic N, Russell A, Pierce DW, Jia Z, McCormick CD, Hartman J, Sakowicz R, Pollard TD. Characterization of two classes of small molecule inhibitors of Arp2/3 complex. Nature. 2009; 460:1031–1034. [PubMed: 19648907]

Pellicena P, Miller WT. Processive phosphorylation of p130Cas by Src depends on SH3-polyproline interactions. The Journal of biological chemistry. 2001; 276:28190–28196. [PubMed: 11389136]

Pellicena P, Stowell KR, Miller WT. Enhanced phosphorylation of Src family kinase substrates containing SH2 domain binding sites. The Journal of biological chemistry. 1998; 273:15325–15328. [PubMed: 9624111]

Quack T, Knobloch J, Beckmann S, Vicogne J, Dissous C, Grevelding CG. The formin-homology protein SmDia interacts with the Src kinase SmTK and the GTPase SmRho1 in the gonads of Schistosoma mansoni. PLoS One. 2009; 4:e6998. [PubMed: 19746159]

Ramalingam N, Zhao H, Breitsprecher D, Lappalainen P, Faix J, Schleicher M. Phospholipids regulate localization and activity of mDia1 formin. Eur J Cell Biol. 2010; 89:723–732. [PubMed: 20619927]

Riento K, Ridley AJ. Rocks: multifunctional kinases in cell behaviour. Nat Rev Mol Cell Biol. 2003; 4:446–456. [PubMed: 12778124]

Roca-Cusachs P, del Rio A, Puklin-Faucher E, Gauthier NC, Biais N, Sheetz MP. Integrin-dependent force transmission to the extracellular matrix by alpha-actinin triggers adhesion maturation. Proc Natl Acad Sci U S A. 2013; 110:E1361–1370. [PubMed: 23515331]

Roca-Cusachs P, Iskratsch T, Sheetz MP. Finding the weakest link: exploring integrin-mediated mechanical molecular pathways. J Cell Sci. 2012; 125:3025–3038. [PubMed: 22797926]

Roskoski R Jr. Src protein-tyrosine kinase structure and regulation. Biochem Biophys Res Commun. 2004; 324:1155–1164. [PubMed: 15504335]

Schonichen A, Mannherz HG, Behrmann E, Mazur AJ, Kuhn S, Silvan U, Schoenenberger CA, Fackler OT, Raunser S, Dehmelt L, et al. FHOD1 is a combined actin filament capping and bundling factor that selectively associates with actin arcs and stress fibers. J Cell Sci. 2013

Schulte A, Stolp B, Schönichen A, Pylypenko O, Rak A, Fackler OT, Geyer M. The human formin FHOD1 contains a bipartite structure of FH3 and GTPase-binding domains required for activation. Structure. 2008; 16:1313–1323. [PubMed: 18786395]

Songyang Z, Shoelson SE, Chaudhuri M, Gish G, Pawson T, Haser WG, King F, Roberts T, Ratnofsky S, Lechleider RJ, et al. SH2 domains recognize specific phosphopeptide sequences. Cell. 1993; 72:767–778. [PubMed: 7680959]

Steffen A, Faix J, Resch GP, Linkner J, Wehland J, Small JV, Rottner K, Stradal TE. Filopodia formation in the absence of functional WAVE- and Arp2/3-complexes. Mol Biol Cell. 2006; 17:2581–2591. [PubMed: 16597702]

Svitkina TM, Borisy GG. Arp2/3 complex and actin depolymerizing factor/cofilin in dendritic organization and treadmilling of actin filament array in lamellipodia. J Cell Biol. 1999; 145:1009–1026. [PubMed: 10352018]

Takeya R, Taniguchi K, Narumiya S, Sumimoto H. The mammalian formin FHOD1 is activated through phosphorylation by ROCK and mediates thrombin-induced stress fibre formation in endothelial cells. EMBO J. 2008; 27:618–628. [PubMed: 18239683]

Thomas SG, Calaminus SD, Machesky LM, Alberts AS, Watson SP. G-protein coupled and IT AM receptor regulation of the formin FHOD1 through Rho kinase in platelets. J Thromb Haemost. 2011; 9:1648–1651. [PubMed: 21605332]

von Wichert G, Jiang G, Kostic A, De Vos K, Sap J, Sheetz MP. RPTP-alpha acts as a transducer of mechanical force on alphav/beta3-integrin-cytoskeleton linkages. J Cell Biol. 2003; 161:143–153. [PubMed: 12682088]

Watanabe N, Kato T, Fujita A, Ishizaki T, Narumiya S. Cooperation between mDia1 and ROCK in Rho-induced actin reorganization. Nat Cell Biol. 1999; 1:136–143. [PubMed: 10559899]

Yamana N, Arakawa Y, Nishino T, Kurokawa K, Tanji M, Itoh RE, Monypenny J, Ishizaki T, Bito H, Nozaki K, et al. The Rho-mDia1 pathway regulates cell polarity and focal adhesion turnover in migrating cells through mobilizing Apc and c-Src. Mol Cell Biol. 2006; 26:6844–6858. [PubMed: 16943426]

Yu CH, Law JB, Suryana M, Low HY, Sheetz MP. Early integrin binding to Arg-Gly-Asp peptide activates actin polymerization and contractile movement that stimulates outward translocation. Proc Natl Acad Sci U S A. 2011; 108:20585–20590. [PubMed: 22139375]

Abbreviations

SFK	Src Family Kinases
FA	focal adhesion
ROCK	Rho Kinase
DID	diaphanous inhibitory domain
DAD	diaphanous autoregulatory domain
RGD	arginine-glycine-aspartic acid peptide
SYF	mouse fibroblast cells deficient in Src, Yes and Fyn
CMV	cytomegalovirus promoter

Highlights

- FHOD1 assembles actin at integrin adhesions to drive cell spreading and migration
- FHOD1-dependent F-actin supports coordinated traction stress and adhesion maturation
- Targeting of FHOD1 to adhesions is controlled by Src Family Kinases
- Correct targeting of FHOD1 is required for subsequent activation by Rho Kinase

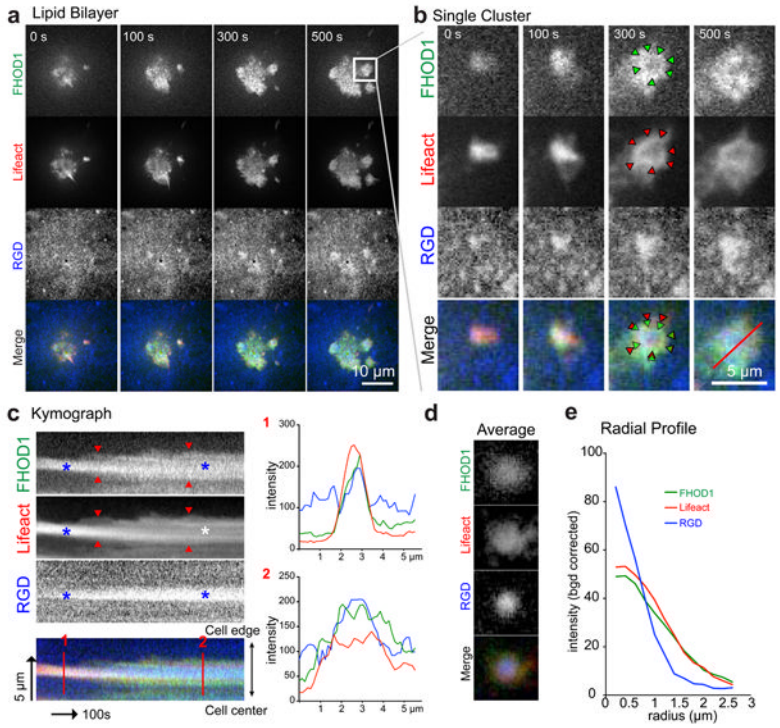

Fig. 1. FHOD1 localizes to early integrin clusters

a) MEF cells were transiently transfected with Ruby-Lifeact and GFP-FHOD1, and then plated onto RGD-membrane labeled with Cascade Blue neutravidin. Ribbon-like actin polymerizes from RGD clusters and expands outwards. FHOD1 is also enriched at RGD clusters. b) Zoom of marked area in (a). Red arrowheads indicate actin ribbon and green arrowheads indicate the intensity maxima of FHOD1-GFP. c) A kymograph of the region marked by the red line in (b) shows early co-localization of both FHOD1 and Lifeact with the RGD clusters (see line profile 1). At later timepoints, Lifeact is localized stronger to the periphery of the cluster and FHOD1 localizes to the center and the periphery of the cluster (line profile 2). Red arrowheads indicate the outwards extending actin and FHOD1; Blue asterisks indicate the RGD cluster and the co-localizing FHOD1 and actin; white asterisks indicate the center of the cluster that is depleted from actin. d) RGD clusters of cells spread for 5 minutes were stacked and averaged with ImageJ. To analyze the enrichement around the clusters, the average pixel intensity outside a circular ROI (radius = 2.5µm) was subtracted (d) and the radial profile was calculated for each channel (e). d-e) n=31 RGD clusters of 7 cells; For mDia1, mDia2 and FMNL3 localization, see Figure S2.

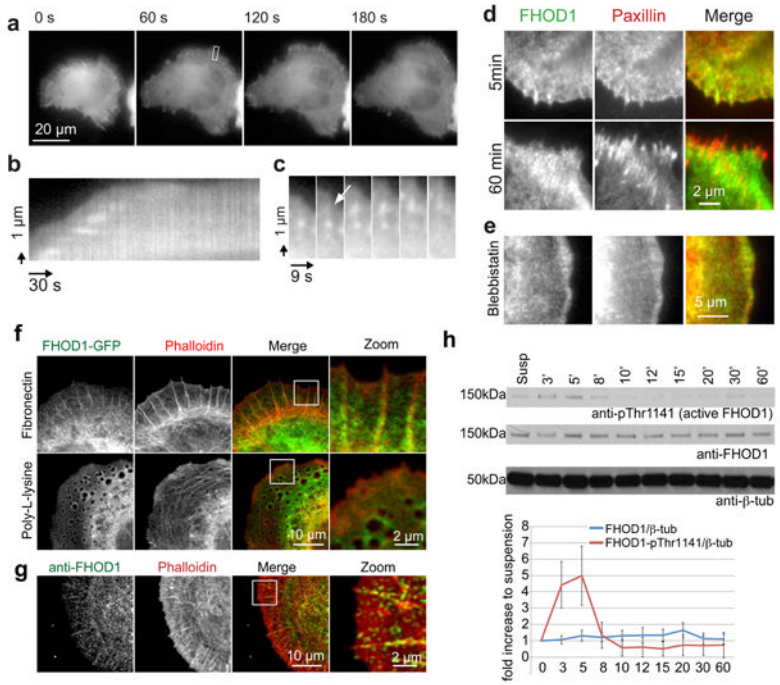

Fig. 2. Active FHOD1 localizes to adhesions on fibronectin coated rigid substrates

a) MEF cells were transfected with FHOD1-GFP and cells were imaged on a TIRF microscope; b) Kymograph of the marked area in (a); c) Time series of the marked area in (a); d) Co-transfection with Paxillin-dsRed shows co-localization at early time points (5 min) and localization of FHOD1 close to adhesions at 60 minutes. e) FHOD1 co-localizes with paxillin also in the absence of myosin II forces (Blebbistatin) f) Localization to the cell edge is lost when cells are plated on Poly-L-lysine. g) The targeting pattern could be confirmed by immunostaining with an anti-FHOD1 antibody. h) FHOD1 activity was tested by western blotting with the phosphospecific anti-FHOD1 pThr1141 antibody that recognizes the active form. Bands were quantified with imageJ. n=3; Error bars indicate standard deviation. See Figure S1 for antibody validation.

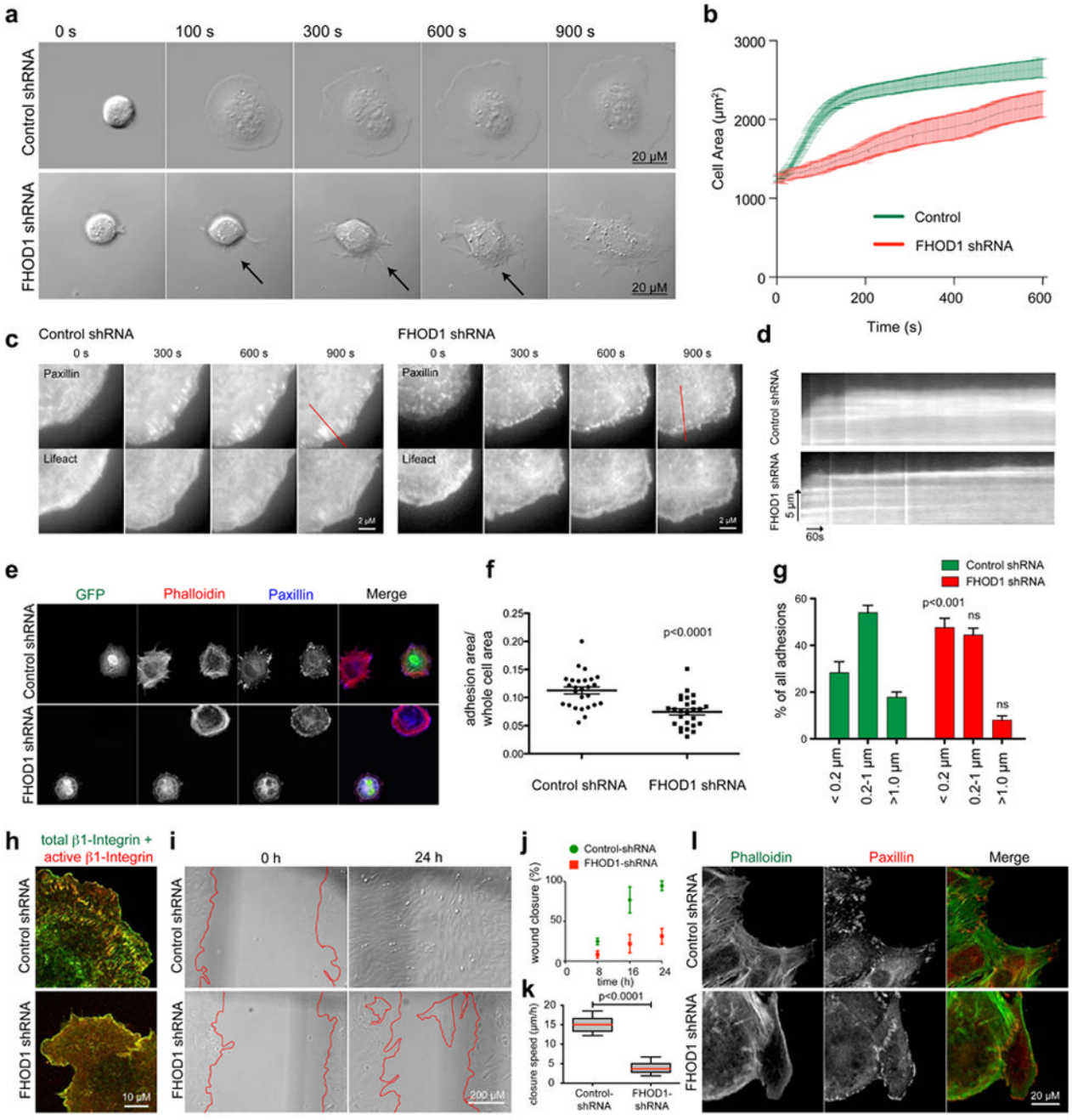

Fig. 3. FHOD1 knockdown disrupts cell spreading

a-b) FHOD1 knockdown cells spread slower. MEF cells were transfected with control shRNA (upper panel) or FHOD1 shRNA plasmids (lower panels) for 72h, plated on fibronectin coated coverslips, identified for knockdown by means of their GFP fluorescence and imaged with a DIC microscope in intervals of 1s (a). Arrows indicate a collapsing protrusion in a knockdown cell. b) Spread area was determined with ImageJ and is shown as the average over n=10 cells, error bars indicate standard error; non-linear regression and comparison between the fitted curves suggests a significant difference with $p<0.0001$. c-d) MEF cells were transfected with control shRNA (upper panel) or FHOD1 shRNA plasmids. After 72h cells were additionally transfected with Paxillin-GFP and pRuby-Lifeact and

imaged by TIRF microscopy in intervals of 3s. While most nascent adhesions mature to focal adhesions (see also (d) for the kymographs of the region marked by the red lines) the nascent adhesion in the knockdown cells do not mature and remain small adhesions that eventually turn over. e-g) Immunostaining of cells after 30 minutes spreading confirms a reduced adhesion area and adhesion maturation in FHOD1 knockdown cells. f) Quantification of the adhesion area as fraction of the whole cell area; n=26 for both conditions. g) The decreased adhesion area is a result of reduced adhesion maturation. Single adhesions (n=2072 and n=1158 from 10 control and FHOD1 shRNA transfected cells, respectively) were measured with imageJ and grouped into three categories (<0.2μm^2, 0.2-1μm^2 and >1μm^2, error bars: SEM). FHOD1 knockdown cells have a significant higher number of nascent (<0.2 μm^2) adhesions (two-way ANOVA and Bonferroni posttest: $p<0.001$). h) Integrin activation at the cell edge is not affected by the FHOD1 knockdown. Green: total β1-Integrin (12G10), red: activated β1-Integrin (9EG7) i-k) FHOD1-shRNA cells are closing wounds more slowly (j: percentage of initial wound, error bars: SEM, k: speed of wound closure in μm/h, error bars: range, n=10). l) FHOD1 knockdown cells are forming only small adhesions at the cell edge during wound closure. Cells were fixed after 8h and stained for Paxillin and F-actin. See also Fig. S3 for the siRNA rescue and Fig. S4 and S5 for the effects of the formin inhibitor smiFH2 on cell spreading and adhesion maturation respectively.

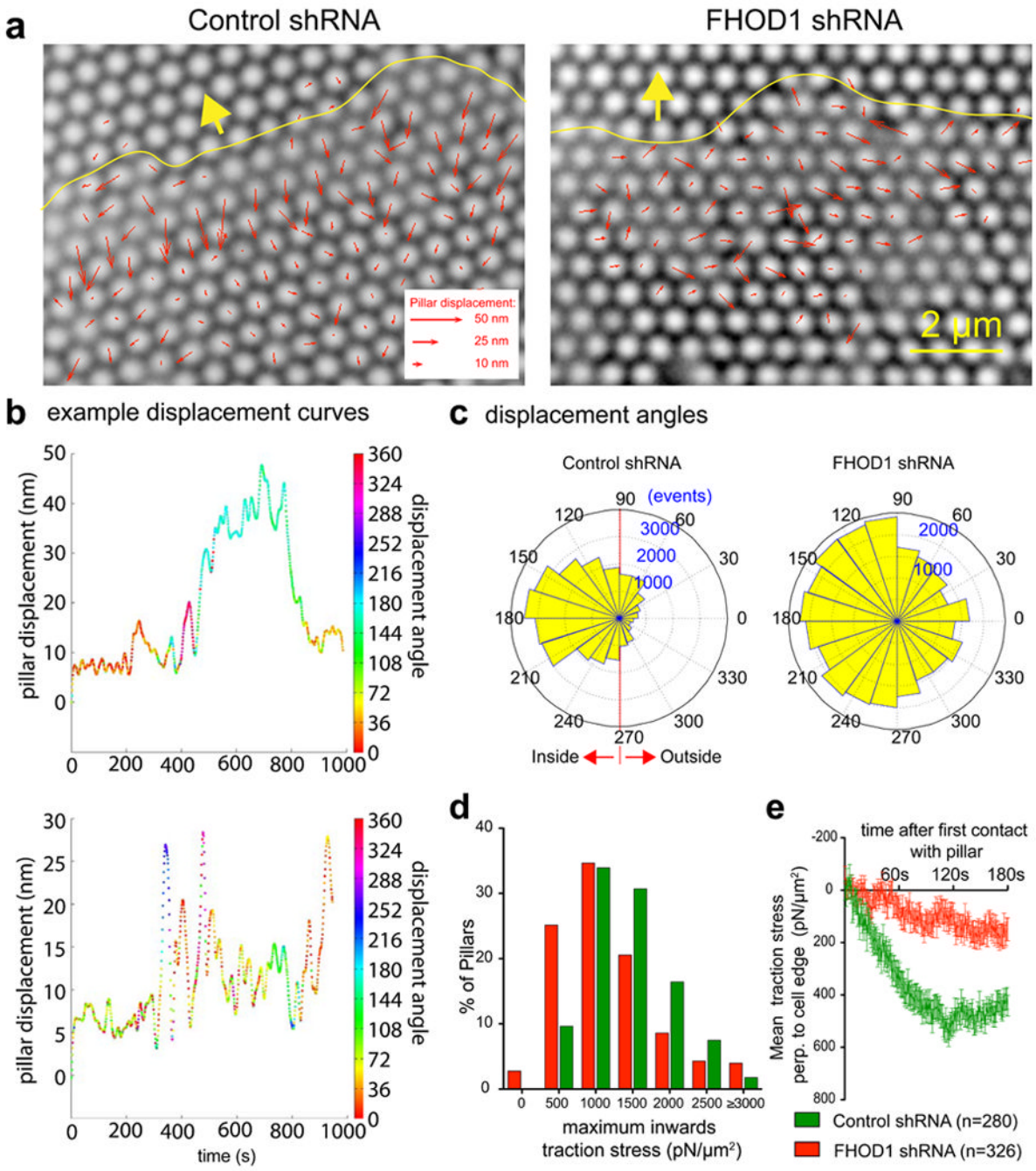

Fig. 4. FHOD1 knockdown abolishes inwards-directed traction stress

Control shRNA and FHOD1-shRNA transfected cells were plated on PDMS pillar arrays (d=0.5µm, h=1.1µm) and imaged on a bright field microscope for ≥15 minutes, from the initiation of spreading, with 1 frame/second. a) Force maps indicate a loss of directed inwards traction after FHOD1 knockdown. Red arrows: pillar displacements, yellow line: cell edge, yellow arrows: protrusion direction; b-c) Angle and magnitude of pillar displacements fluctuate in FHOD1 knockdown cells (see example curves with color-coded displacement angles in (b)) and pillar displacement angles are widely distributed (c). As a result, the maximum inwards stress per pillar is reduced, as well ($p<0.0001$) (d) and there is a striking loss of the overall mean inwards stress (e). The two data sets are statistically

different (Non-linear regression and comparison of fits: $p<0.0001$) c-e) n=280 and 326 pillars from 5 cells each, for the control and the FHOD1 knockdown, respectively. Displacement angles are all displacements over noise level (i.e. 10 nm) for 3 minutes after first contact with the cell edge (Control: n=35,196, FHODl-shRNA: n=36,872 events).

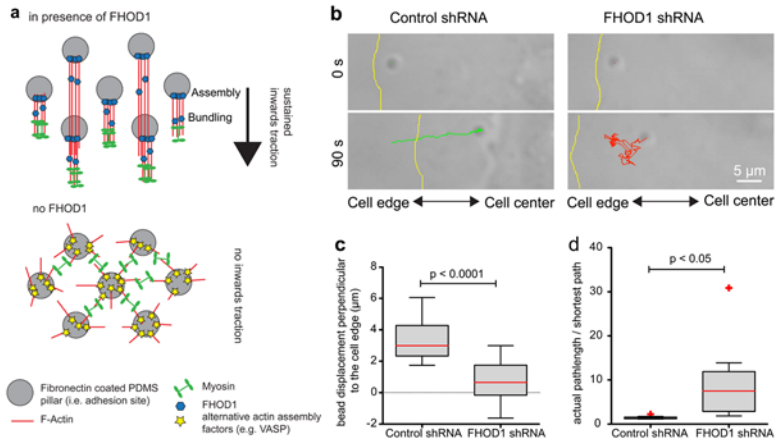

Fig. 5. FHOD1 knockdown impairs the retrograde flow

a) Working model: FHOD1 assembles actin filaments from integrin adhesion sites (e.g. pillar tops that are coated with fibronectin) and partially moves with the polymerizing actin to bundle the filaments into higher ordered structures. Myosin pulling is directed, resulting in inwards-traction and retrograde flow. In the absence of FHOD1 actin filaments are still formed by alternative actin assembly proteins, such as VASP or ARP2/3 but to lesser extent. Also, the filaments lack organization, allowing the myosins to pull from multiple directions, thus cancelling out the forces and retrograde flow. b-d) Displacement analysis of fibronectin coated beads (1 µm diameter) shows a reduced retrograde flow (c) and strongly increase off-axis movement (d) after 90 seconds (because of the fast displacements in control cells, inwards movement stopped after ~ 90 seconds in some cases), thus supporting the working model (c,d: n=10, p values from student's t-test). Note that the Cell edge retraction in the Control shRNA cell (b) is the result of a typical retraction/protrusion cycle that started approx. 50 seconds after the imaging (see also Movie 7).

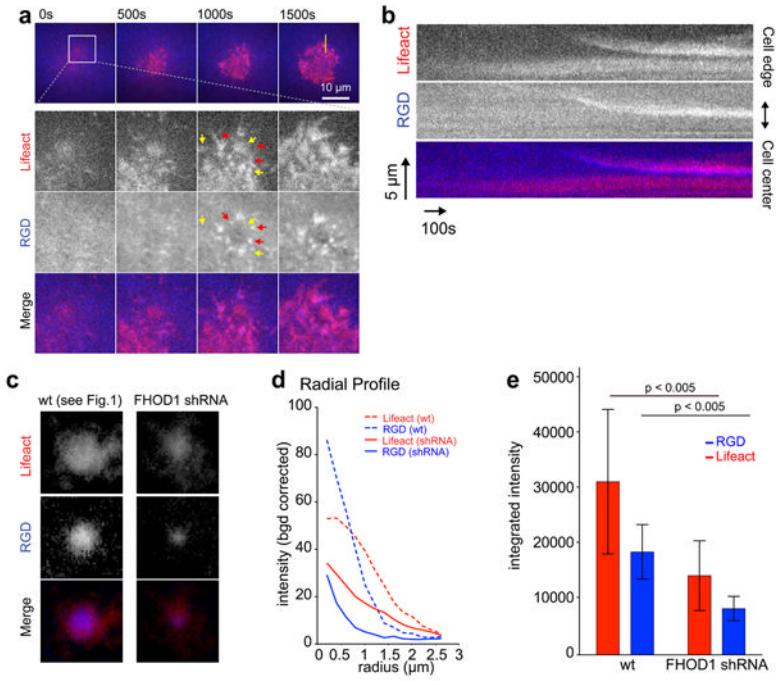

Fig. 6. FHOD1 knockdown disrupts actin assembly from integrin clusters and cluster growth on lipid bilayer

a) Mouse embryonic fibroblasts were transfected with FHOD1 shRNA and Ruby-lifeact and plated on RGD-supported membrane. Due to the small size of the RGD clusters, a Kalman filter (imageJ) was applied to the RGD channel. Red arrows indicate RGD clusters without actin, while yellow arrows show actin accumulations outside of RGD clusters. b) Kymograph of the region marked by a yellow line in (a); c-e) Averaging of the RGD clusters suggests reduced cluster size and F-actin around the RGD clusters (images of the average over 31 wt (see also Fig 1) and 47 FHOD1 shRNA clusters are shown in (c) and the radial profiles are shown in (d). e) The integrated intensity of a ROI with a radius of 2.5μm was measured with imageJ. The graph shows the average and error bars show the standard deviation over n=7 cells for both conditions. Student's t-tests confirm a significant reduction in both F-actin and RGD levels around the cluster center.

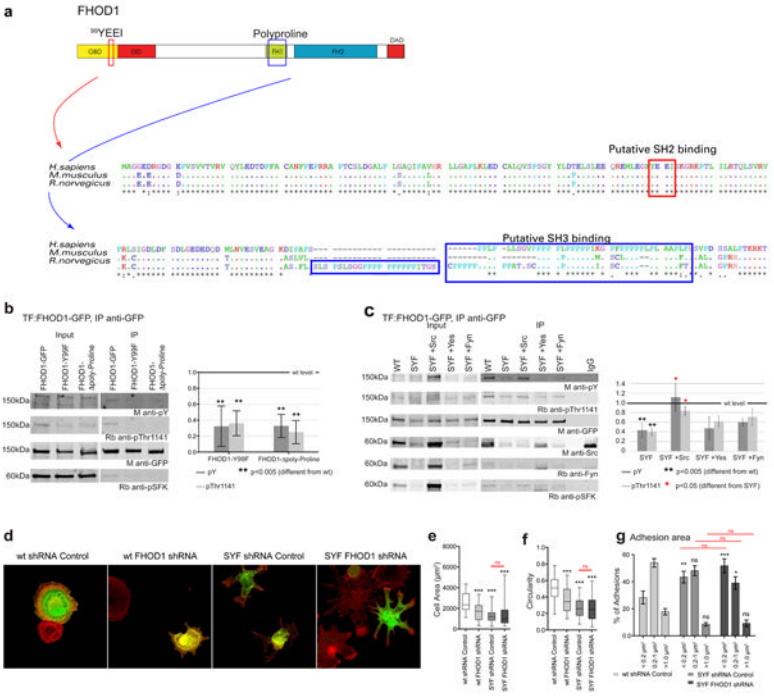

Fig. 7. FHOD1 is phosphorylated by SFKs

a) Schematic of FHOD1 and the putative SH2 and SH3 binding sites and alignment of human (H. sapiens), mouse (M. musculus) and rat (R. norvegicus) FHOD1 sequences. b) Immunoprecipitated wild type FHOD1, but not the Y99F or the poly-proline deletion (FHOD1-Δpoly-proline) construct shows a band when probed with an anti-phospho-tyrosine antibody. Similarly a band with the phospho-Thr1141 antibody can be detected only on wild type FHOD1 and interaction with SFKs (anti-pSFK) is reduced or abolished for FHOD1-Y99F and FHOD1-Δpoly-proline, respectively c) Tyrosine phosphorylation and Thr1141 phosphorylation are reduced in SYF cells, but can be restored by Src (b,c: n=3, error bars indicate standard deviation). Incubation with Src, Fyn or pSFK antibodies suggest interaction with Src, Yes and Fyn. d-h) SYF cells spread slower (d,e) and have irregular cell shapes (d,f). However, the phenotype is not aggravated by FHOD1 knockdown (error bars: range). Similarly SYF cells have a reduced adhesion area (g) and more immature adhesions after 30 minutes spreading (h), irrespective of FHOD1 levels. p values from student's t-test (e-g) or two-way ANOVA with Bonferroni posttests (h): error bars: SEM, *p<0.05; **p<0.005; ***p<0.001; ns: not significant; results from t-tests between SYF shRNA control and SYF FHOD1 shRNA are shown in red. See also Fig. S6 for PP2 treatment.

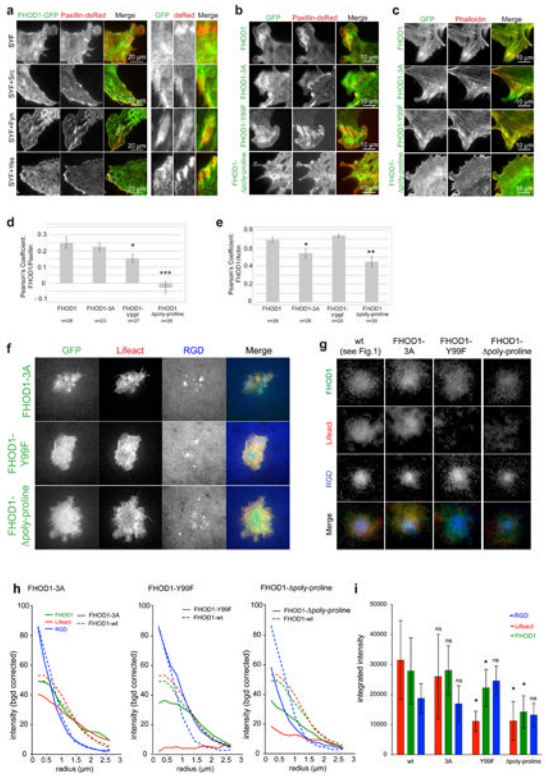

Fig. 8. FHOD1 is recruited to adhesions downstream of SFKs

a) FHOD1 localization to adhesions is lost in SYF cells, but can be restored by the re-introduction of Src, Yes, or Fyn; SYF cells or add-back cells for the indicated kinase were co-transfected with FHOD1-GFP and Paxillin-dsRed and imaged by TIRF microscopy. b) TIRF microscopy shows localization of wt-FHOD1, constitutive inactive FHOD1 (FHOD1-3A) and the Y99F-mutant, but not FHOD1-Δpoly-proline to the adhesion region (quantification of co-localization in d). c) All FHOD1 constructs localized to actin filaments, but with FHOD1-3A or FHOD1-Δpoly-proline the correlation was reduced (e). f-i) Wild type FHOD1 and constitutive inactive FHOD1-3A, but not FHOD1-Y99F or FHOD1-Δpoly-proline localize to RGD clusters; Representative images of cells that were spread on the bilayers for five minutes. g) Average over RGD clusters (after five minutes spreading) of cells transfected with the indicated constructs; h) Radial profile of the average clusters and i) the average integrated intensity (error bars indicate standard deviation) of clusters of single cells (n=7 cells for wt, 5 for FHOD1-3A and FHOD1-Δpoly-proline and 4 cells for FHOD1-Y99F).